Journal of Ayurveda and Integrative Medicine 13 (2022) 100449

Contents lists available at ScienceDirect

Journal of Ayurveda and Integrative Medicine

journal homepage: http://elsevier.com/locate/jaim

Original Research Article (Experimental)

Evaluation of potency of the selected bioactive molecules from Indian medicinal plants with M^{Pro} of SARS-CoV-2 through in silico analysis

Pinku Halder [a], Upamanyu Pal [a], Pranab Paladhi [a], Saurav Dutta [a], Pallab Paul [a], Samudra Pal [a], Debasmita Das [a], Agnish Ganguly [a], Ishita Dutta [a], Sayarneel Mandal [a], Anirban Ray [b], Sujay Ghosh [a, *]

[a] Cytogenetics & Genomics Research Unit, Department of Zoology; University of Calcutta, Taraknath Palit Siksha Prangan (Ballygunge Science College Campus), 35 Ballygunge Circular Road, Kolkata, West Bengal, 700019, India
[b] Department of Zoology, Bangabasi Morning College (affiliated to University of Calcutta), Kolkata, West Bengal, 700009, India

ARTICLE INFO

Article history:
Received 16 July 2020
Received in revised form
12 April 2021
Accepted 5 May 2021
Available online 21 May 2021

Keywords:
SARS CoV-2 virus
M^{pro}
In silico molecular docking
Phytochemical
Indian spices
Medicinal plants

ABSTRACT

Background: The recent outbreak of the novel SARS-CoV-2 across the globe and the absence of specific drug against this virus lead the scientific community to look into some alternative indigenous treatments. India as a hub of Ayurvedic and medicinal plants can shed light on its treatment using specific active bio-molecules from these plants.
Objectives: Keeping our herbal resources in mind, we were interested to inquire whether some phytochemicals from Indian spices and medicinal plants can be used as alternative therapeutic agents in contrast to synthetic drugs.
Materials and methods: We used *in silico* molecular docking approach to test whether bioactive molecules of herbal origin such as hyperoside, nimbaflavone, ursolic acid, 6-gingerol, 6-shogaol and 6-paradol, curcumin, catechins and epigallocatechin, α-Hederin, piperine could bind and potentially block the M^{pro}enzyme of the SARS-CoV-2 virus.
Results: Ursolic acid showed the highest docking score (−8.7 kcal/mol) followed by hyperoside (−8.6 kcal/mol), α-Hederin (−8.5 kcal/mol) and nimbaflavone (−8.0 kcal/mol). epigallocatechin, catechins, and curcumin also exhibited high binding affinity (Docking score −7.3, −7.1 and −7.1 kcal/mol) with the M^{pro}. The remaining tested phytochemicals exhibited moderate binding and inhibitory effects.
Conclusion: This finding provides a basis for biochemical assay of tested bioactive molecules on SARS-CoV-2 virus.

1. Introduction

The Severe Acute Respiratory Syndrome Coronavirus 2 (SARS-CoV-2) is a highly infectious virus for novel coronavirus disease -19 (COVID-19) disease that caused the recent outbreak in China in December 2019 and rapidly spread to the other parts of the globe owing to its extreme contagious nature. Its initial symptoms include fever, dry cough, tiredness, aches or pains, diarrhoea, difficulty in breathing, etc. In the human body, it probably settles through the angiotensin-converting enzyme 2 (ACE2) [1] receptor for entry into the host cell and the transmembrane protease, serine 2 (TMPRSS2) for viral spike protein priming [2,3]. The infection gradually took the shape of a pandemic with extremely high mortality [4,5] owing to lack of definite treatment regimen and medications against the virus as well as due to the presence of co-morbidities. Even the so-called developed nations like U.S and several European countries failed to control the infection with their cutting-edge medical technologies at a very early phase. As a result, the World Health Organisation declared COVID-19 as a public health emergency of international concern [6].

The previous name of this betacoronavirus was 2019-nCoV. It was renamed as SARS-CoV-2 by the International Committee on Taxonomy of Viruses (ICTV) [7]. The genome of SARS-CoV-2 has been sequenced [8]. The whole genome sequence analysis of SARS-

* Corresponding author.
E-mail address: sgzoo@caluniv.ac.in (S. Ghosh).
Peer review under responsibility of Transdisciplinary University, Bangalore.

https://doi.org/10.1016/j.jaim.2021.05.003

CoV-2 shows 96.2% similarity with bat coronavirus (SARSr-Co) [9,10], while it shows low sequence identity with that of SARS-CoV (about 79%) or MERS-CoV (about 50%) [11,12].

Since, the onset of the COVID-19 pandemic, globally, researchers are involved in the rapid development of drugs and specific antiviral treatment strategies. Among all the SARS-CoV-2 targets the main protease (M^{pro}, $3CL^{pro}$, nsp5) of the virus received major attention [13,14]. Some alternative targets like spike protein (S), RNA-dependent RNA-polymerase (RdRp, nsp12), NTPase/helicase (nsp13) and papain-like protease (PL^{pro}, part of nsp3) have also been reported in some literature [15,16]. The SARS-CoV-2 M^{pro} is a 33.8 kDa enzyme which plays a pivotal role in the cleavage of viral polyproteins (pp1a and pp1ab) in a site-specific (L-Q (S, A, G)) manner [17], resulting in the release of functional replicase enzyme which is crucial for transcription and replication of the virus [18–20]. Other essential enzymes which are involved in the replication process such as RdRp or nsp13 cannot fully function without this proteolytic action [13], making M^{pro} a key enzyme in viral replication cycle. As a result, the inhibition of M^{pro} could stop viral replication process and thus alleviate disease symptoms [21,22]. For drug discovery against SARS-CoV-2 virus, M^{pro} is one of the most attractive viral targets. Some studies have already reported synthetic competitive inhibitors against SARS-CoV-2 M^{pro} [17,23,24]; however, increase in substrate concentration often reduces the effectiveness of such inhibitors. Natural phytochemicals can provide safe and effective treatment by alleviating this limitation.

Although there are no approved drugs for COVID-19, a number of clinical trials are in progress [25]. Lopinavir and ritonavir, combined with Chinese herbal medicines, were used in preliminary clinical studies [26].

Indian medicinal plants and spices are a rich hub of ingredients which can be utilized for drug designing because of their high therapeutic values [27]. Previous docking study already reported that phytochemicals such as hyperoside and nimbaflavone are good candidate drugs against influenza virus strains [28]. A recent study has suggested high binding efficacy of ursolic acid (*Tulsi*) against surface spike glycoprotein and RNA polymerase of SARS-CoV-2 virus [29]. Ajoene and allicin (Garlic) shows strong virucidal activity against selected viruses including, herpes simplex virus type 1, herpes simplex virus type 2, parainfluenza virus type 3, vaccinia virus, vesicular stomatitis virus, and human rhinovirus type 2 [30]. Curcumin has diverse antiviral activity against dengue virus, herpes simplex virus, Zika and chikungunya virus [31–33]. Previous study reported that catechins and epigallocatechin form green tea leaves have profound antiviral effects [34]. A very recent *in silico* molecular docking study revealed that piperine from black pepper can act as a potent inhibitor of the antiviral enzymes of dengue and Ebola viruses [35].

Molecular docking is a computational technique, widely used for the study of molecular recognition, prediction of binding mode and binding affinity of complexes formed by two or more known structures. It has become a widely accepted tool for drug discovery [36–40]. This high throughput technique can screen a variety of available drugs to identify potential drugs for novel diseases as well as to predict the adverse effects of novel drugs in a very short time [41–44]. Development of novel drugs is a time-consuming process and generally several years of work is required for clinical approval [45]. Drug repositioning, also known as repurposing, is an effective strategy to combat novel diseases caused by infectious agents that spread rapidly [46–48]. Drugs that have been approved for some disease, are safe for human use [49], and only their effectiveness against the disease of interest needs to be established [50]. In life-threatening cases, where there is no alternative medicine or vaccine, such drug repurposing strategy is particularly attractive. However, clinical trials are necessary to ensure that such treatment is better than a placebo [51,52].

An *in silico* screening of herbal medicines for treatment of COVID-19 has also been reported [53]. Although several clinical trials are in progress to assess the potential effects of putative therapeutic agents, very limited data is available publicly regarding the *in vitro* and *in vivo* activities of the drugs that are currently involved in clinical trials for treatment of COVID-19 [25]. It has been reported that chloroquine phosphate shows anti-COVID-19 activity [54]. Several clinical trials are assessing the potential of protease inhibitors such as lopinavir and ritonavir that have been approved for treatment of other viral infections. Lopinavir and ritonavir were identified in earlier studies to target the M^{pro} of the SARS virus.

In the present study, we utilized the recently available high resolution experimental structure of the main protease (M^{pro}) of SARS-CoV-2 (Fig. 1) [55], as the target for molecular docking-based virtual screening. The predictions of this study will provide information that can be utilized for choice of candidate drugs for *in vitro*, *in vivo* and clinical trials.

2. Materials and methods

2.1. Protein and chemical compounds

The X-ray crystal structure of COVID-19 M^{pro} in complex with an inhibitor N3 (PDB ID: 6LU7) [56], having 2.16 Å resolution was downloaded from RCSB Protein Data Bank (PDB) [57]. We collected Simplified Molecular Input Line Entry System (SMILES) code for 15 ligand molecules and then 3D structures were generated and downloaded in PDB format from CORINAClassic (https://www.mn-am.com/online_demos/corina_demo).

For hyperoside and nimbaflavone, SMILE codes were downloaded from Neem Metabolites Structure Database [58]. For rest of the ligands, SMILE codes were collected from DrugBank (https://www.drugbank.ca/) and PubChem (https://pubchem.ncbi.nlm.nih.gov/).

This *in silico* study was carried out by using AutoDock suite 4.2.6 for protein and ligand preparations, PyRx 0.8 for grid generation and protein-ligand docking, PyMol V1.7.4 (Educational use only) and Discovery Studio 2.5.5 for visualization of docking result and Ligplot + version 1.4.5 for generation of 2D Ligplot. The entire computational study was done in Windows 8.1 operating system.

2.2. Protein preparation

SARS-CoV-2 M^{pro} was prepared for molecular docking study by using AutoDock suite 4.2.6 software. Protein preparation wizard has the following steps: removal of water molecules, removal of inhibitor N3 from protein structure to obtained fresh protein for docking, addition of polar hydrogens, and addition of Kollman charges. After preparation protein molecule was exported in Protein Data Bank, Partial Charge (Q), & Atom Type (T) (PDBQT) format from AutoDock.

2.3. Ligand preparation

All 15 ligands (Fig. 1) were prepared for docking using AutoDock suite 4.2.6 software. Ligand preparation has the following steps: addition of hydrogen atoms, removal of unwanted molecules, addition of all hydrogens, computation of Gasteiger charges, merging of non-polar hydrogens, generating ionization states at pH 7, tautomers, geometric characteristics, and low-energy ring conformations. After preparation, ligand molecules were exported in PDBQT format for docking in PyRx 0.8 software.

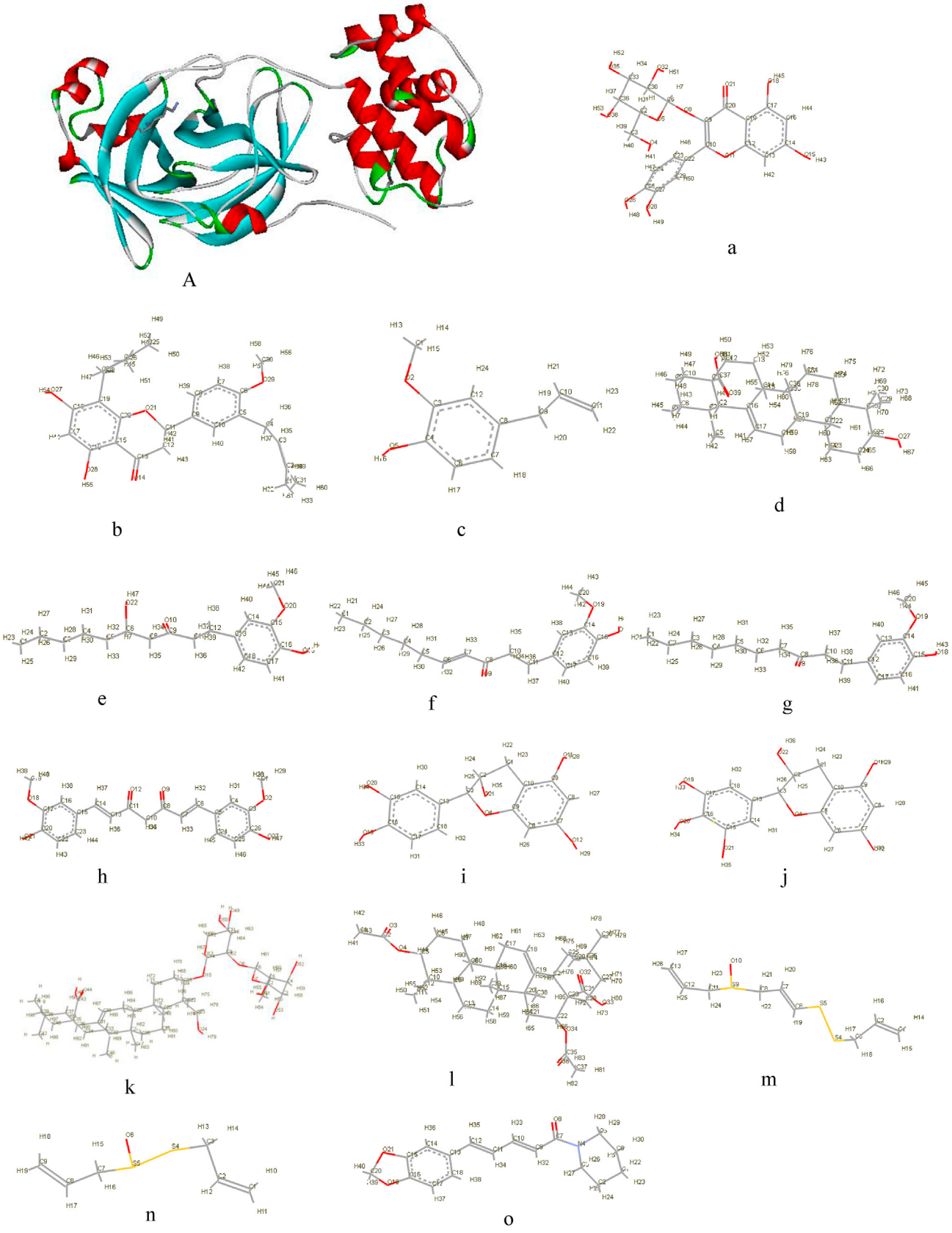

Fig. 1. 3D cartoon structure of SARS-CoV-2 main protease and all 15 ligands in stick form. A) Main protease a) Hyperoside b) Nimbaflavone c) Eugenol d) Ursolic acid ; e) 6-gingerol f) 6-shogaol g) 6-paradol h) Curcumin i) Catechins j) Epigallocatechin k) α-Hederin l) Echinocystic acid diacetate m) Ajoene n) Allicin o) Piperine.

Table 1
Summary of all 15 bioactive compounds screened against SARS CoV-2 M^{pro} with their respective source, binding energy, interacting residues and inhibition constant.

Compounds	Source	SMILE code collected from	AutoDock Binding Energy ΔGb (kcal/mol)	No. of H-bonds	Interacting Residues	Inhibition constant (Ki) (nM)
Hyperoside	*Neem (Azadirachta indica)*	Neem Metabolite Structure Database	−8.6	6	Leu141[a], Ser144[a], His163[a], Arg188[a], Thr190[a], Gln192	494.36
Nimbaflavone	*Neem (Azadirachta indica)*	Neem Metabolite Structure Database	−8	1	His163[a]	1370.95
Eugenol	Clove (*Syzygium aromaticum*)	DrugBank, DB09086	−4.9	6	Leu141[a], Gly143, Ser144[a], Cys145, His163[a]	256085.29
Ursolic acid	*Tulsi* or holy basil (*Ocimum sanctum*)	Drugbank, DB15588	−8.7	3	Thr24, Leu141[a], Ser144[a]	421.27
6-gingerol	Ginger *(Zingiber officinale)*	PubChem, 442793	−5.8	5	Arg188[a], Gln189, Thr190[a], Gln192	56008.89
6-shogaol	Ginger *(Zingiber officinale)*	PubChem, 5281794	−5.8	4	Arg188[a], Thr190[a], Gln192	56008.89
6-paradol	Ginger *(Zingiber officinale)*	PubChem, 94378	−5.7	5	Glu166, Arg188, Thr190[a], Gln192	66387.61
Curcumin	Turmeric *(Curcuma longa)*	DrugBank, DB11672	−7.1	4	Gly143, Ser144[a]	6268.33
Catechins	Tea plant *(Camellia sinensis)*	PubChem, 1203	−7.1	2	Thr26, Gln189	6268.33
Epigallocatechin	Tea plant *(Camellia sinensis)*	DrugBank, DB03823 (EXPT01331)	−7.3	7	Leu141[a], Ser144[a], Cys145, His163[a]	4461.61
α-Hederin	Black cumin *(Nigella sativa)*	PubChem, 73296	−8.5	4	His163[a], Glu166[a], Gln189	585.97
Echinocystic acid diacetate	Sponge gourd *Luffa cylindrica*	PubChem, 476534	−6.7	1	Glu166	12249.81
Ajoene	Garlic *(Allium sativum)*	PubChem, 5386591	−4.1	–	–	987829.94
Allicin	Garlic *(Allium sativum)*	DrugBank, DB11780	−3.6	2	Ser144[a], Cys145	2288176.65
Piperine	Black pepper (*Piper nigrum*)	DrugBank, DB12582	−6.8	3	Thr25, Ser144[a], Cys145	10334.73

-: Nil.
[a] Hotspot residue.

2.4. Grid generation

The grid generation process was done in PyRx 0.8 software. It provided a square block at the active site of the protein for the accurate binding score with thermodynamic optimal energy. A grid box size of x = 27.9382928446, y = 28.2467551684, and z = 30.0038760533 Å points was generated to cover active amino acid residues that are important for docking [55]. The grid was centered at x,y,z coordinates of −13.9467660792, 12.664485092, 68.4908850063.

2.5. Molecular docking

Molecular docking was conducted with PyRx 0.8 software which uses AutodockVina wizard at the backend. 15 ligands were docked with generated grid of prepared protein. The exhaustiveness parameter that controls the extent of the search was chosen as 8, and 9 modes were generated for each ligand. The best ligand pose selection for the receptor was done based on the docking score and lowest Root Mean Square Deviation (RMSD) value.

2.6. Validation of docking score

For validation of docking results, we used another web server Webina 1.0.2 by Durrant Lab [59] with exactly same parameters. The best ligand pose selection for the receptor was done based on the docking score and lowest RMSD value.

2.7. Calculation of inhibition constant [K_i] from binding energy

After docking, best ligand poses for all 15 ligands were selected on the basis of binding energy ΔGb (kcal/mol) and RMSD values. Then inhibition constant (K_i) (nM) were calculated from binding energy.

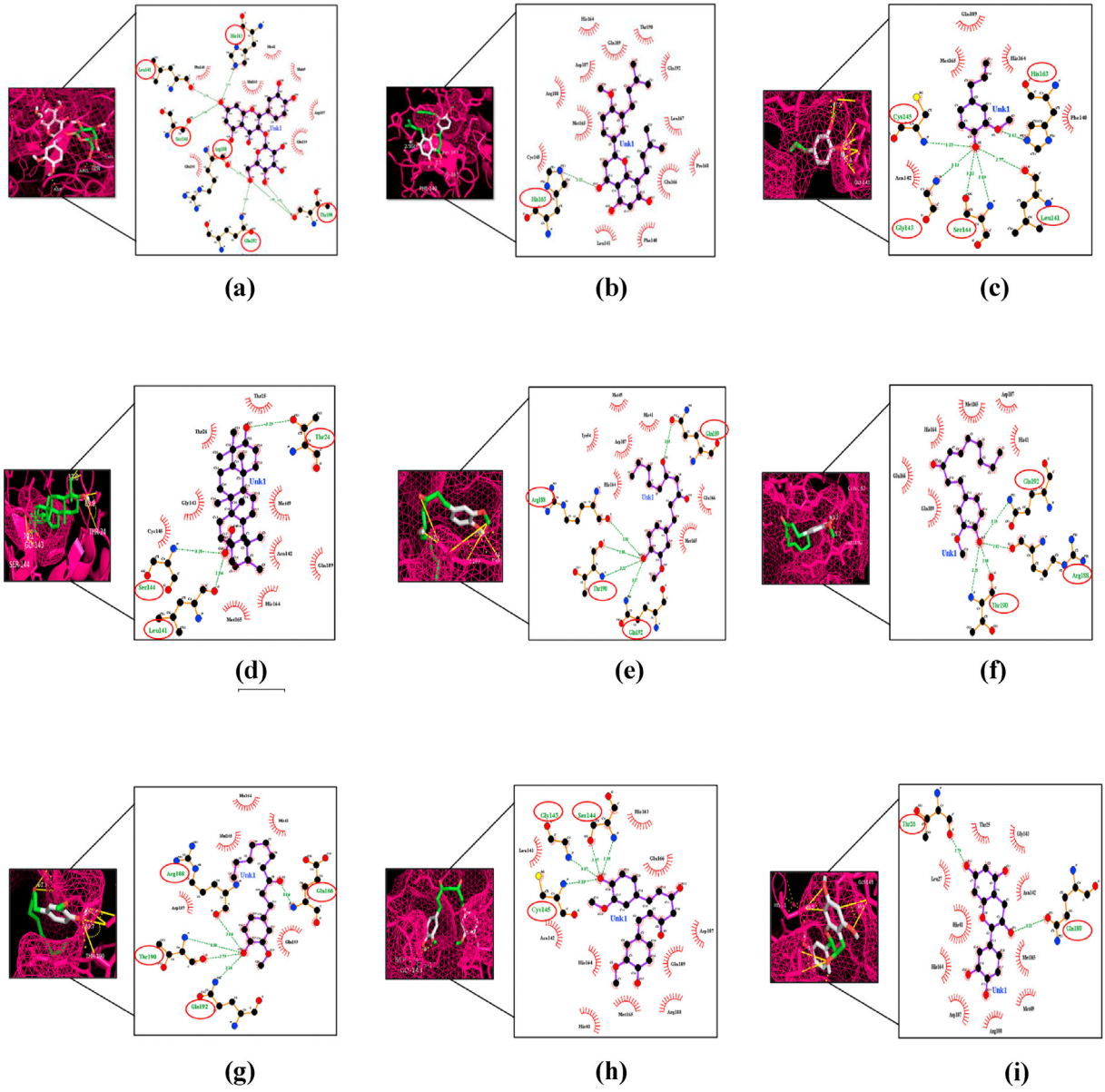

Fig. 2. The binding site of SARS CoV-2 M^{pro}, represented as a mesh, shows ligand interactions. Amino acid residues that formed polar H-bonds with ligands are highlighted with red circle in Ligplot. (a) Hyperoside (b) Nimbaflavone (c) Eugenol (d) Ursolic acid (e) 6-gingerol (f) 6-shogaol (g) 6-paradol (h) Curcumin (i) Catechins.

2.8. Molecular dynamics simulation study

The protein and docked protein-ligand complexes were subjected to Molecular Dynamics (MD) Simulation using MDWeb web portal [60]. GROMACS FULL MD setup was performed using AMBER-99SB* force field. Simple Box Solvent Molecular Dynamics (NPT) operations were performed using the following settings: Total time 2 fs, Temperature 300 K, Total time 10 ns, Output frequency 500 steps and Total 10,000 snapshots, to obtained MD trajectory file. Water molecules and ions were removed from trajectories to obtained dry trajectory. The RMSD and B-factor fluctuations along the residues were calculated for the protein and all docked protein-ligand complexes and plotted to compare the protein backbone stability. Due to limitation in computing power, no further analyses were performed.

3. Results

This study was done to identify possible compounds that can bind to the M^{pro}, which may be used as a potential drug target for SARS-CoV-2. We tested 15 bioactive compounds from Indian spices and medicinal plants that have been previously reported for their antiviral activity [28,31,34,61–65]. These compounds can bind with the M^{pro} with a docking score of −8.7 to −3.6 kcal/mol (Table 1). Ursolic acid (Drugbank ID DB15588), a compound of *Tulsi*, reported to have antiviral activity [29], had highest docking score −8.7 (kcal/mol) than others (Table 1), and formed three hydrogen bonds (H-bonds) with Thr24, Leu141*, Ser144* residues of M^{pro} (Fig. 2). Hyperoside and nimbaflavone were predicted to have a docking score of −8.6 and −8.0 kcal/mol (Table 1). Hyperoside forms six H-bonds with Leu141*, Ser144*, His163*, Arg188*, Thr190*, Gln192

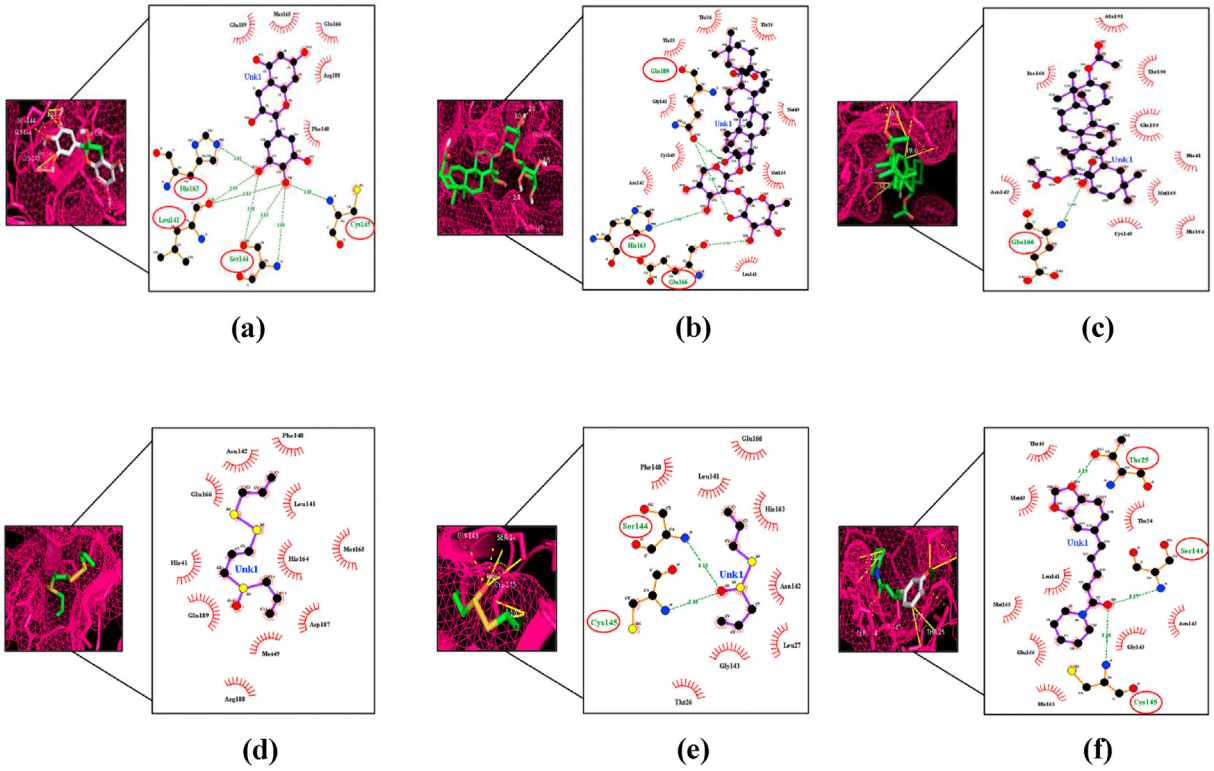

Fig. 3. The binding site of SARS CoV-2 M^{pro}, represented as a mesh, shows ligand interactions. Amino acid residues that formed polar H-bonds with Ligands are highlighted with red circle in Ligplot. (a) Epigallocatechin (b) α-Hederin (c) Echinocystic acid diacetate (d) Ajoene (e) Allicin (f) Piperine.

residues whereas nimbaflavone exhibited single H-bond with His163* residue of SARS-CoV-2 M^{pro} (Fig. 2). Eugenol (DrugBank ID DB09086), the principal bioactive compound of clove, exhibited a docking score of −4.9 kcal/mol (Table 1), and formed six H-bonds with Leu141*, Gly143, Ser144*, Cys145, His163* residues of viral M^{pro} (Fig. 2). Natural compounds of ginger i.e., 6-gingerol (PubChem ID 442793), 6-shogaol (PubChem ID 5281794) and 6-paradol (PubChem ID 94378) were predicted to have a docking score of −5.8, −5.8 and −5.7 kcal/mol (Table 1). 6-Gingerol forms five interacting H-bonds with Arg188*, Gln189, Thr190*, Gln192 residues, 6-shogaol forms four interacting H-bonds with three residues of SARS-CoV-2 M^{pro} (Arg188*, Thr190*, Gln192), whereas 6-paradol exhibited five interacting H-bonds with Glu166, Arg188*, Thr190*, Gln192 residues of the viral M^{pro} (Fig. 2). Curcumin (DrugBank ID

Table 2
Predicted binding affinity of all 15 tested phytochemicals and Quercetin, Remdesivir, PF-00835231 against SARS-CoV-2 M^{pro}.

Compound	AutoDock Binding Energy ΔGb (kcal/mol)	No. of H-bonds	Interacting Residues	Inhibition constant (Ki) (nM)
Ursolic acid	−8.7	3	Thr24, Leu141[a], Ser144[a]	421.27
Hyperoside	−8.6	6	Leu141[a], Ser144[a], His163[a], Arg188[a], Thr190[a], Gln192	494.36
α-Hederin	−8.5	4	His163[a], Glu166, Gln189	585.97
PF-00835231	−8.4	8	His41, Leu141[a], Gly143[a], Ser144[a], Cys145, Gln189	3764.107
Nimbaflavone	−8	1	His163[a]	1370.95
Remdesivir	−7.7	5	Phe140, Leu141[a], Gly143[a], Ser144[a], His163[a]	2260.33
quercetin	−7.4	8	Leu141[a], Gly143[a], Ser144[a], Cys145, His163[a]	694.55
Epigallocatechin	−7.3	7	Leu141[a], Ser144[a], Cys145, His163[a]	4461.61
Curcumin	−7.1	4	Gly143[a], Ser144[a]	6268.33
Catechins	−7.1	2	Thr26, Gln189	6268.33
Piperine	−6.8	3	Thr25, Ser144[a], Cys145	10334.73
Echinocystic acid diacetate	−6.7	1	Glu166	12249.81
6-gingerol	−5.8	5	Arg188[a], Gln189, Thr190[a], Gln192	56008.89
6-shogaol	−5.8	4	Arg188[a], Thr190[a], Gln192	56008.89
6-paradol	−5.7	5	Glu166, Arg188[a], Thr190[a], Gln192	66387.61
Eugenol	−4.9	6	Leu141[a], Gly143, Ser144[a], Cys145, His163[a]	256085.29
Ajoene	−4.1	Nil	Nil	987829.94
Allicin	−3.6	2	Ser144[a], Cys145	2288176.65

[a] Hotspot residue.

Table 3
Predicted binding energies (Kcal/mol) of all 15 phytochemicals and 3 compounds in PyRx 0.8 and Webina 1.0.2

Compounds	Binding Energy ΔGb (kcal/mol)	
	Docking with PyRx 0.8	Docking with Webina 1.0.2
Hyperoside	−8.6	−8.6
Nimbaflavone	−8	−8
Eugenol	−4.9	−4.9
Ursolic acid	−8.7	−8.7
6-gingerol	−5.8	−5.6
6-shogaol	−5.8	−5.8
6-paradol	−5.7	−5.3
Curcumin	−7.1	−6.9
Catechins	−7.1	−7.1
Epigallocatechin	−7.3	−7.3
α-Hederin	−8.5	−8.6
Echinocystic acid diacetate	−6.7	−6.9
6-gingerol	−4.1	−4.2
6-shogaol	−3.6	−3.5
6-paradol	−6.8	−7
Ajoene	−4.9	−4.9
Allicin	−4.1	−4.1
Piperine	−3.6	−3.7
quercetin	−7.4	−7.4
Remdesivir	−7.7	−7.6
PF-00835231	−8.4	−8.4

DB11672), the active compound of turmeric, had a docking score of −7.1 kcal/mol (Table 1) and formed four H-bonds with two interacting residues of M^{pro} (Gly143*, Ser144*) (Fig. 2). Two main naturally occurring compounds of tea plant, catechins (PubChem ID 1203) and epigallocatechin (DrugBank ID DB03823), predicted to have a docking score of −7.1 kcal/mol and −7.3 kcal/mol respectively (Table 1). Catechins formed two H-bonds with Thr26, Gln189 residues (Fig. 2) of viral M^{pro} whereas epigallocatechin exhibited seven interacting H-bonds with Leu141*, Ser144*, Cys145, His163* residues of M^{pro} (Fig. 3). α-Hederin (PubChemID73296), had a significantly higher docking score of −8.5 kcal/mol (Table 1), and formed four interacting H-bonds with His163*, Glu166, Gln189 residues of SARS-CoV-2 M^{pro} (Fig. 3). Echinocystic acid diacetate (PubChem ID 476534), a triterpenoid saponin compound, had a docking score prediction of −6.7 kcal/mol (Table 1), and exhibited single interacting H-bond with Glu166 residue of M^{pro} (Fig. 3). Two main natural compounds of garlic i.e, ajoene (PubChem ID 5386591) and allicin (DrugBank ID DB11780) were predicted to have a docking score of −4.1 kcal/mol and −3.6 kcal/mol (Table 1). Allicin formed two interacting H-bonds with Ser144*, Cys145 residues of M^{pro} whereas ajoene did not form any H-bond with SARS-CoV-2 M^{pro} (Fig. 3). Piperine (DrugBank ID DB12582), a naturally occurring bioactive compound of black pepper, had a docking score prediction −6.8 kcal/mol (Table 1). Piperine formed three interacting H-bonds with Thr25, Ser144*, Cys145 residues of viral M^{pro} (Fig. 3). Docking results were validated by Webina 1.0.2 web server using the same docking parameters. Not much significant difference was observed between binding affinity predictions by PyRx 0.8 and Webina 1.0.2 web server by Durrant lab (Table 3).

We selected all 15 ligands to simulate using MDWeb web portal [60]. To evaluate the stability of protein-ligand complexes, the RMSD of the protein backbone and protein-ligand complex were calculated during a 10 ns MD trajectory. The RMSD fluctuation per residue showed that protein-ligand complexes were stable (Fig. 4A) which indicates that the protein-ligand complexes remain intact during simulation process. As shown in Fig. 4A most of the values of RMSD were fluctuated between 0.4 Å and 1.2 Å, with an average of 0.7 Å.

For further analysis of residual atomic flexibility, an isotropic temperature factor (B-factor) was calculated. B-factor generally reflects the mobility of each residue around its mean position. It is an important tool for analysing the dynamic stability during MD simulation process. Fig. 4B shows B-factor fluctuation per residue of protein and all protein-ligand complexes. Based on the general trend of change, B-factor fluctuation of protein-ligand complexes are nearly similar to that of protein backbone; however, some residues show higher flexibility. As shown in Fig. 4B, B-factor values were fluctuated between 5 $Å^2$and 15 $Å^2$ with an average of 9 $Å^2$. Detailed information regarding the same has been provided in the Supplementary Tables S1 and S2.

3.1. Predicted binding affinity of all 15 phytochemicals compared to quercetin, remdesivir and PF-00835231 against SARS-CoV-2 M^{pro}

We compared docking results of all 15 phytochemicals with three well-known drugs viz., quercetin (DrugBank ID DB04216), remdesivir (DrugBank ID DB14761), and PF-00835231 (PubChem CID 11561899) that can target SARS-CoV-2 M^{pro} (Table 2). Quercetin had a docking score prediction −7.4 kcal/mol. Remdesivir was predicted to have a docking score of −7.7 kcal/mol. PF-00835231 compound exhibited high binding affinity for M^{pro} (−8.4 kcal/mol). Comparison of the docking results of all 15 phytochemicals showed that ursolic acid (−8.7 kcal/mol), hyperoside (−8.6 kcal/mol) and α-Hederin (−8.5 kcal/mol) have greater binding affinity with M^{pro} of SARS-CoV-2 virus than quercetin, remdesivir and PF-00835231, which are currently being used in COVID-19 treatment (Table 2).

4. Discussion

In this study, we evaluated the efficacy of 15 bioactive compounds from Indian spices and medicinal plants as potential inhibitors of SARS-CoV-2 M^{pro}. All these compound have some antiviral properties as reported in published literature. Hyperoside, a neem secondary metabolite, has potential effects against influenza virus nucleoprotein [28]. Ursolic acid exhibits strong antiviral activity against rotavirus [66]. 6-Gingerol and 6-paradol show high efficacy against hepatitis C virus [67]. Green tea catechins and epigallocatechin have been reported to have antiviral effects against numerous viruses such as herpes simplex virus, hepatitis B virus, hepatitis C virus, etc. [34]. Previous study reported that eugenol can inhibit human herpes virus *in vitro* and *in vivo* [62]. Curcumin can inhibit Zika and chikungunya viruses [31]. Garlic compound allicin is highly effective against human cytomegalovirus, influenza B, herpes simplex virus type 1, herpes simplex virus type 2 [68].

The molecular docking approach provides an opportunity to test different drugs against SARS-CoV-2 M^{pro} in combination with N3 inhibitor. Recent docking study showed that the inhibitor N3 can bind to the substrate binding pockets of new COVID-19 M^{pro} [56]. This substrate binding pockets are located within a cleft between domain I and II and are highly conserved among all SARS-CoV-2 M^{pro}s which make it a good target for designing drugs for anti-COVID-19 activity [56]. Similarly, we analysed the above mentioned bioactive compounds from Indian spices and medicinal plants which may act as potential drug targets for SARS-CoV-2 M^{pro}. Out of the 15 bioactive compounds, 9 exhibited very high docking scores (scores > −6.5 kcal/mol) (Table 1). Highest docking score was exhibited by ursolic acid (−8.7 kcal/mol) which is the principal bioactive compound of *Tulsi* leaf extract. The α-Hederin exhibited second highest docking score of −8.5 kcal/mol (Table 1). *Neem* secondary metabolites, hyperoside and nimbaflavone exhibited

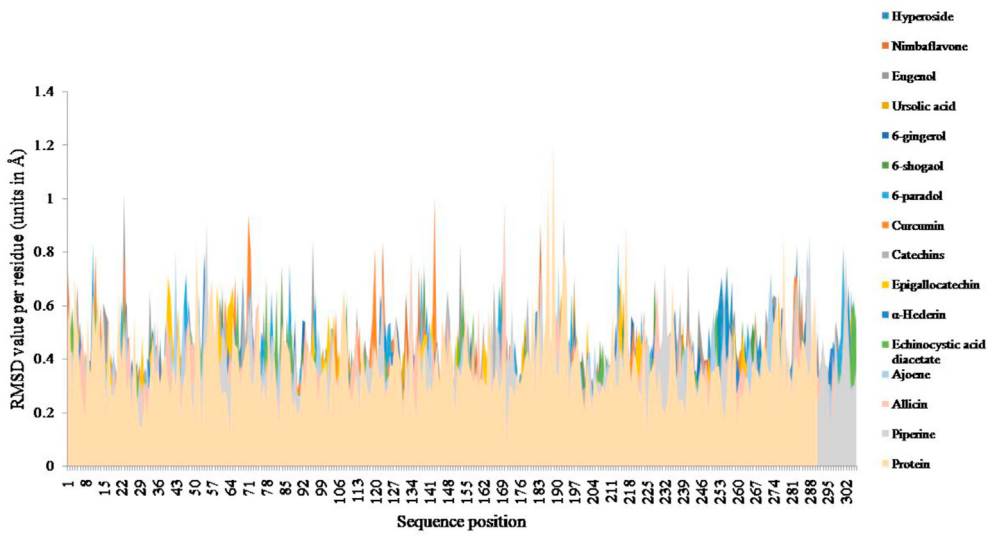

A

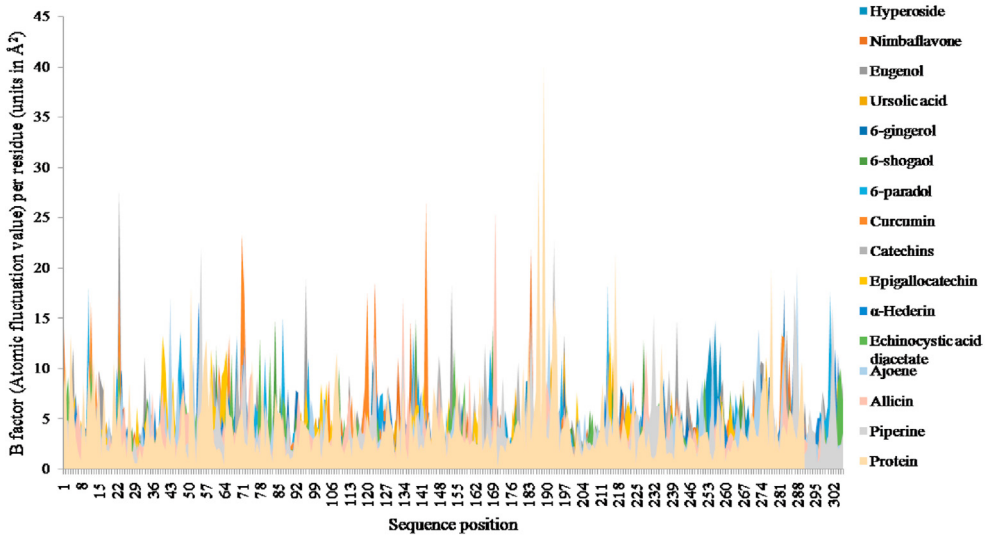

B

Fig. 4. A) Plots of Root Mean Square Deviation (RMSD) fluctuations per residue in Protein and all 15 protein-ligand complexes. B) Plots of B-factor fluctuations per residue in Protein and all 15 protein-ligand complexes.

docking score as −8.6 and −8.0 kcal/mol (Table 1). Curcumin exhibited docking score of −7.1 kcal/mol (Table 1). Compounds of tea plant i.e., catechins and epigallocatechin exhibited a docking score of −7.1 kcal/mol and −7.3 kcal/mol respectively (Table 1). Piperine, the bioactive compound from black pepper yielded docking score −6.8 kcal/mol (Table 1). Echinocystic acid diacetate yielded docking score −6.7 kcal/mol (Table 1). We identified five hotspot residues namely Leu141, Ser144, His163, Arg188, Thr190 (Table 1) on the sequence of SARS-CoV-2 M^{pro}which exhibited effective interaction with all the tested bioactive compounds. These residues can be targeted for potential drug designing to block SARS-CoV-2 M^{pro}. In addition, we compared (Table 2) the binding capacity of these tested bioactive compounds with widely used popular drugs against SARS-CoV-2 infection across the world. These widely used drugs are quercetin, remdesivir, PF-00835231. Interestingly, three of our tested compounds namely ursolic acid, hyperoside, α-hederin exhibited stronger binding and inhibitory potential against SARS-CoV-2 M^{pro} compared to quercetin, remdesivir, PF-00835231.

Our study suffers from some potential limitations. It would have been better to use GROMACS full package for entire molecular dynamics simulation analyses. We did not use MM/PBSA and MM/GBSA program for calculating free binding energy calculation of each bioactive compound. We could not determine the inhibitory effects in term of IC50 value for each of these tested drug. Moreover, our finding needs wet lab experimental validation.

5. Conclusion

In the present study, we selected and tested 15 bioactive compounds against SARS-CoV-2 M^{pro}. These compounds are found among Indian spices and medicinal plants and exhibit antiviral properties. Among them, nine compounds namely ursolic acid, α-Hederin, hyperoside, nimbaflavone, curcumin, catechins, epigallocatechin, piperine, and echinocystic acid diacetate exhibited very high docking score against SARS-CoV-2 M^{pro}. We also identified a set of hotspot residues on the peptide chain of the viral protease which are important for protein-ligand interactions and can be targeted for designing novel drugs against SARS-CoV-2 M^{pro}. Moreover, through comparative analyses we demonstrated that three bioactive agents have higher potential to inhibit the SARS-CoV-2 M^{pro}, than the drugs that are being used widely across the globe in treatment of COVID19. This comparative analyses makes us optimistic to develop herbal drugs without any side-effects in near future. This is particularly important as many cases have been reported from across the globe regarding secondary drug complications among the patients following recovery from SARC-CoV-2 infection. Our study will help researchers to carry similar analyses for other drugs and Ayurvedic bioactive agents and all these would contribute effectively to win the battle against SARS-CoV-2 infections.

Source(s) of funding

The work is financially supported by Department of Science and Technology, Government of West Bengal, India, Grant no. SG/WBDST/S&T 1000114/2016.

Conflict of interest

None.

Acknowledgement

The infrastructural support and instrumental facilities were provided by **UGC-UPE II, DST-FIST, UGC-PURSE** program at University of Calcutta. Pinku Halder is thankful to University Grants Commission, Government of India for providing him NET-JRF fellowship for his research.

Appendix A. Supplementary data

Supplementary data to this article can be found online at https://doi.org/10.1016/j.jaim.2021.05.003.

References

[1] Li W, Moore MJ, Vasilieva N, Sui J, Wong SK, Berne MA, et al. Angiotensin-converting enzyme 2 is a functional receptor for the SARS coronavirus. Nature 2003;426(6965):450–4.
[2] Matsuyama S, Nagata N, Shirato K, Kawase M, Takeda M, Taguchi F. Efficient activation of the severe acute respiratory syndrome coronavirus spike protein by the transmembrane protease TMPRSS2. J Virol 2010;84(24):12658–64.
[3] Glowacka I, Bertram S, Müller MA, Allen P, Soilleux E, Pfefferle S, et al. Evidence that TMPRSS2 activates the severe acute respiratory syndrome coronavirus spike protein for membrane fusion and reduces viral control by the humoral immune response. J Virol 2011;85(9):4122–34.
[4] Wu F, Zhao S, Yu B, Chen Y-M, Wang W, Song Z-G, et al. A new coronavirus associated with human respiratory disease in China. Nature 2020;579(7798):265–9.
[5] Zhao S, Lin Q, Ran J, Musa SS, Yang G, Wang W, et al. Preliminary estimation of the basic reproduction number of novel coronavirus (2019-nCoV) in China, from 2019 to 2020: a data-driven analysis in the early phase of the outbreak. Int J Infect Dis 2020;92:214–7.
[6] Lai C-C, Shih T-P, Ko W-C, Tang H-J, Hsueh P-R. Severe acute respiratory syndrome coronavirus 2 (SARS-CoV-2) and coronavirus disease-2019 (COVID-19): the epidemic and the challenges. Int J Antimicrob Agents 2020;55(3):105924.
[7] Coronaviridae Study Group of the International Committee on Taxonomy of Viruses. The species Severe acute respiratory syndrome-related coronavirus: classifying 2019-nCoV and naming it SARS-CoV-2. Nat Microbiol 2020;5(4):536–44. https://doi.org/10.1038/s41564-020-0695-z.
[8] Yadav PD, Potdar VA, Choudhary ML, Nyayanit DA, Agrawal M, Jadhav SM, et al. Full-genome sequences of the first two SARS-CoV-2 viruses from India. Indian J Med Res 2020;151(2 & 3):200–9.
[9] Zhou P, Yang X-L, Wang X-G, Hu B, Zhang L, Zhang W, et al. A pneumonia outbreak associated with a new coronavirus of probable bat origin. Nature 2020;579(7798):270–3.
[10] Paraskevis D, Kostaki EG, Magiorkinis G, Panayiotakopoulos G, Sourvinos G, Tsiodras S. Full-genome evolutionary analysis of the novel corona virus (2019-nCoV) rejects the hypothesis of emergence as a result of a recent recombination event. Infect Genet Evol 2020;79:104212.
[11] Lu R, Zhao X, Li J, Niu P, Yang B, Wu H, et al. Genomic characterisation and epidemiology of 2019 novel coronavirus: implications for virus origins and receptor binding. Lancet 2020;395(10224):565–74.
[12] Tang X, Wu C, Li X, Song Y, Yao X, Wu X, et al. On the origin and continuing evolution of SARS-CoV-2. Natl Sci Rev 2020;7(6):1012–23. https://doi.org/10.1093/nsr/nwaa036.
[13] Thiel V, Ivanov KA, Putics Á, Hertzig T, Schelle B, Bayer S, et al. Mechanisms and enzymes involved in SARS coronavirus genome expression. J Gen Virol 2003;84(Pt 9):2305–15.
[14] Yang H, Yang M, Ding Y, Liu Y, Lou Z, Zhou Z, et al. The crystal structures of severe acute respiratory syndrome virus main protease and its complex with an inhibitor. Proc Natl AcadSci USA 2003;100(23):13190–5.
[15] Hilgenfeld R, Peiris M. From SARS to MERS: 10 years of research on highly pathogenic human coronaviruses. Antivir Res 2013;100(1):286–95.
[16] Wu C, Liu Y, Yang Y, Zhang P, Zhong W, Wang Y, et al. Analysis of therapeutic targets for SARS-CoV-2 and discovery of potential drugs by computational methods. Acta Pharm Sin B 2020;10(5):766–88. https://doi.org/10.1016/j.apsb.2020.02.008.
[17] Ma C, Sacco MD, Hurst B, Townsend JA, Hu Y, Szeto T, et al. Boceprevir, GC-376, and calpain inhibitors II, XII inhibit SARS-CoV-2 viral replication by targeting the viral main protease. Cell Res 2020;30(8):678–92.
[18] Ziebuhr J, Snijder EJ, Gorbalenya AE. Virus-encoded proteinases and proteolytic processing in the Nidovirales. J Gen Virol 2000;81(Pt 4):853–79.
[19] Hegyi A, Ziebuhr J. Conservation of substrate specificities among coronavirus main proteases. J Gen Virol 2002;83(Pt 3):595–9.
[20] Du Q-S, Wang S-Q, Zhu Y, Wei D-Q, Guo H, Sirois S, et al. Polyprotein cleavage mechanism of SARS CoVMpro and chemical modification of the octapeptide. Peptides 2004;25(11):1857–64.
[21] Liang P-H. Characterization and inhibition of SARS-coronavirus main protease. Curr Top Med Chem 2006;6(4):361–76.
[22] Yang H, Bartlam M, Rao Z. Drug design targeting the main protease, the Achilles' heel of coronaviruses. Curr Pharmaceut Des 2006;12(35):4573–90.
[23] Zhu L, George S, Schmidt MF, Al-Gharabli SI, Rademann J, Hilgenfeld R. Peptide aldehyde inhibitors challenge the substrate specificity of the SARS-coronavirus main protease. Antivir Res 2011;92(2):204–12.
[24] Zhang L, Lin D, Sun X, Curth U, Drosten C, Sauerhering L, et al. Crystal structure of SARS-CoV-2 main protease provides a basis for design of improved α-ketoamide inhibitors. Science 2020;368(6489):409–12.
[25] Lu H. Drug treatment options for the 2019-new coronavirus (2019-nCoV). Biosci Trends 2020;14(1):69–71.
[26] Wang Z, Chen X, Lu Y, Chen F, Zhang W. Clinical characteristics and therapeutic procedure for four cases with 2019 novel coronavirus pneumonia receiving combined Chinese and Western medicine treatment. Biosci Trends 2020;14(1):64–8.
[27] Introduction and importance of medicinal plants and herbs National Health Portal of India. Available from: https://www.nhp.gov.in/introduction-and-importance-of-medicinal-plants-and-herbs-mtl.
[28] Ahmad A, Javed MR, Rao AQ, Husnain T. Designing and screening of universal drug from neem (Azadirachtaindica) and standard drug chemicals against influenza virus nucleoprotein. BMC Compl Alternative Med 2016;16(1):519.
[29] Kumar AH. Molecular docking of natural compounds from Tulsi (ocimum sanctum) and neem (azadirachtaindica) against SARS-CoV-2 protein targets. BEMS Reports 2020;6(1):11–3.
[30] Weber ND, Andersen DO, North JA, Murray BK, Lawson LD, Hughes BG. In vitro virucidal effects of Allium sativum (garlic) extract and compounds. Planta Med 1992;58(5):417–23.
[31] Mounce BC, Cesaro T, Carrau L, Vallet T, Vignuzzi M. Curcumin inhibits Zika and chikungunya virus infection by inhibiting cell binding. Antivir Res 2017;142:148–57.
[32] Padilla-S L, Rodríguez A, Gonzales MM, Gallego GJC, Castaño OJC. Inhibitory effects of curcumin on dengue virus type 2-infected cells in vitro. Arch Virol 2014;159(3):573–9.

[33] Kutluay SB, Doroghazi J, Roemer ME, Triezenberg SJ. Curcumin inhibits herpes simplex virus immediate-early gene expression by a mechanism independent of p300/CBP histone acetyltransferase activity. Virology 2008;373(2):239–47.
[34] Xu J, Xu Z, Zheng W. A review of the antiviral role of green tea catechins. Molecules 2017;22(8):1337. https://doi.org/10.3390/molecules22081337.
[35] Nag A, Chowdhury RR. Piperine, an alkaloid of black pepper seeds can effectively inhibit the antiviral enzymes of Dengue and Ebola viruses, an in silico molecular docking study. Virusdisease 2020;31(3):308–15.
[36] Marshall GR. Computer-aided drug design. Annu Rev Pharmacol Toxicol 1987;27:193–213.
[37] Leelananda SP, Lindert S. Computational methods in drug discovery. Beilstein J Org Chem 2016;12:2694–718.
[38] Kuntz ID. Structure-based strategies for drug design and discovery. Science 1992;257(5073):1078–82.
[39] Macalino SJY, Gosu V, Hong S, Choi S. Role of computer-aided drug design in modern drug discovery. Arch Pharm Res (Seoul) 2015;38(9):1686–701.
[40] Talluri S. Computational protein design of bacteriocins based on structural scaffold of aureocin A53. Int J Bioinf Res Appl 2019;15(2):129.
[41] Jones G, Willett P, Glen RC, Leach AR, Taylor R. Development and validation of a genetic algorithm for flexible docking. J Mol Biol 1997;267(3):727–48.
[42] Friesner RA, Banks JL, Murphy RB, Halgren TA, Klicic JJ, Mainz DT, et al. Glide: a new approach for rapid, accurate docking and scoring. 1. Method and assessment of docking accuracy. J Med Chem 2004;47(7):1739–49.
[43] Irwin JJ, Shoichet BK. Docking screens for novel ligands conferring new biology. J Med Chem 2016;59(9):4103–20.
[44] Mohanasundaram N, Sekhar T. Computational studies of molecular targets regarding the adverse effects of isoniazid drug for tuberculosis. Curr Pharmacogenomics Personalized Med (CPPM) 2019;16(3):210–8.
[45] Fons N. Focus: drug development: textbook of drug design and discovery, fifth edition. Yale J Biol Med 2017;90(1):160.
[46] Ashburn TT, Thor KB. Drug repositioning: identifying and developing new uses for existing drugs. Nat Rev Drug Discov 2004;3(8):673–83.
[47] Li J, Zheng S, Chen B, Butte AJ, Swamidass SJ, Lu Z. A survey of current trends in computational drug repositioning. Briefings Bioinf 2016;17(1):2–12.
[48] Chopra G, Samudrala R. Exploring polypharmacology in drug discovery and repurposing using the CANDO platform. Curr Pharmaceut Des 2016;22(21):3109–23.
[49] Li H, Wang YM, Xu JY, Cao B. [Potential antiviral therapeutics for 2019 novel coronavirus]. Zhonghua Jiehe He Huxi Zazhi 2020;43(3):170–2. https://doi.org/10.3760/cma.j.issn.1001-0939.2020.03.004.
[50] Hurle MR, Yang L, Xie Q, Rajpal DK, Sanseau P, Agarwal P. Computational drug repositioning: from data to therapeutics. Clin Pharmacol Ther 2013;93(4):335–41.
[51] Ding X. Drug screening: drug repositioning needs a rethink. Nature 2016;535(7612):355.
[52] Novac N. Challenges and opportunities of drug repositioning. Trends Pharmacol Sci 2013;34(5):267–72.
[53] Zhang D-H, Wu K-L, Zhang X, Deng S-Q, Peng B. In silico screening of Chinese herbal medicines with the potential to directly inhibit 2019 novel coronavirus. J Integr Med 2020;18(2):152–8.
[54] Gao J, Tian Z, Breakthrough Yang X. Chloroquine phosphate has shown apparent efficacy in treatment of COVID-19 associated pneumonia in clinical studies. Biosci Trends 2020;14(1):72–3.
[55] Jin Z, Du X, Xu Y, Deng Y, Liu M, Zhao Y, et al. Structure of M^{pro} from COVID-19 virus and discovery of its inhibitors. BioRxiv 2020. https://doi.org/10.1101/2020.02.26.964882.
[56] Jin Z, Du X, Xu Y, Deng Y, Liu M, Zhao Y, et al. Structure of Mpro from SARS-CoV-2 and discovery of its inhibitors. Nature 2020;582(7811):289–93. https://doi.org/10.1038/s41586-020-2223-y.
[57] Burley SK, Berman HM, Kleywegt GJ, Markley JL, Nakamura H, Velankar S. Protein data bank (PDB): the single global macromolecular structure archive. Methods Mol Biol 2017;1607:627–41.
[58] Hatti KS, Muralitharan L, Hegde R, Kush A. Neemdb: convenient database for neem secondary metabolites. Bioinformation 2014;10(5):314–5.
[59] Kochnev Y, Hellemann E, Cassidy KC, Durrant JD. Webina: an open-source library and web app that runs AutoDockVina entirely in the web browser. Bioinformatics 2020;36(16):4513–5. https://doi.org/10.1093/bioinformatics/btaa579.
[60] Hospital A, Andrio P, Fenollosa C, Cicin-Sain D, Orozco M, Gelpí JL. MDWeb and MDMoby: an integrated web-based platform for molecular dynamics simulations. Bioinformatics 2012;28(9):1278–9.
[61] Chang JS, Wang KC, Yeh CF, Shieh DE, Chiang LC. Fresh ginger (Zingiber-officinale) has anti-viral activity against human respiratory syncytial virus in human respiratory tract cell lines. J Ethnopharmacol 2013;145(1):146–51.
[62] Cortés-Rojas DF, de Souza CRF, Oliveira WP. Clove (Syzygiumaromaticum): a precious spice. Asian Pac J Trop Biomed 2014;4(2):90–6.
[63] Astani A, Reichling J, Schnitzler P. Screening for antiviral activities of isolated compounds from essential oils. Evid Based Complement Alternat Med 2011;2011:253643. https://doi.org/10.1093/ecam/nep187.
[64] Mikaili P, Maadirad S, Moloudizargari M, Aghajanshakeri S, Sarahroodi S. Therapeutic uses and pharmacological properties of garlic, shallot, and their biologically active compounds. Iran J Basic Med Sci 2013;16(10):1031–48.
[65] Prasad S, Tyagi AK. Ginger and its constituents: role in prevention and treatment of gastrointestinal cancer. Gastroenterol Res Pract 2015;2015:142979.
[66] Tohmé MJ, Giménez MC, Peralta A, Colombo MI, Delgui LR. Ursolic acid: a novel antiviral compound inhibiting rotavirus infection in vitro. Int J Antimicrob Agents 2019;54(5):601–9.
[67] Abd El-Wahab A, El-Adawi H, El-Demellawy M. In vitro study of the antiviral activity of Zingiberofficinale. Planta Med 2009;75(9). https://doi.org/10.1055/s-0029-1234649.
[68] Ankri S, Mirelman D. Antimicrobial properties of allicin from garlic. Microb Infect 1999;1(2):125–9.